

**MATHEMATICAL MODELLING OF  
IONICITY FACTOR AND BULK MODULUS FOR  
HEXAGONAL BINARY SEMICONDUCTOR  
MATERIALS**

**GHASSAN EZZULDDIN ARIF**

**UNIVERSITISAINSMALAYSIA**

**2015**

**MATHEMATICAL MODELLING OF  
IONICITY FACTOR AND BULK MODULUS FOR  
HEXAGONAL BINARY SEMICONDUCTOR  
MATERIALS**

by

**GHASSAN EZZULDDIN ARIF**

Thesis submitted in fulfillment of the  
requirements for the degree of Doctor of  
Philosophy

March 2015



## **ACKNOWLEDGEMENTS**

### **In the Name of Allah, Most Gracious, Most Merciful**

Throughout my thesis process, I would like to express my gratitude to everyone who has supported me in every way and provided inspiration to make my study an unforgettable experience. First and foremost, I would like to thank Allah, without Whom I would not have been able to complete this endeavor. Likewise, I wish to express my heartfelt gratitude to my supervisors Dr. Farah Aini Binti Abdullah and Assoc. Prof. Dr. Yarub Al-Douri, who have given generously of their knowledge and time, and their encouraging comments and feedback on my work have been a great inspiration and helped me in countless ways.

With great pleasure, I would like to express my sincere thanks to the Universiti Sains Malaysia for the great opportunity of study and for the academic facilities that they have offered me. I would like to acknowledge the help of the libraries of Universiti Sains Malaysia that has provided me with the most valuable sources and books. Special thanks go to the school of Mathematical Sciences and its labs for the immense help in accomplishing this thesis.

Despite the long physical distance, whereby most of our communication has been over the phone, the love and encouragement of my brothers, Ihssan, Mukdad, Anas, and my only one sister, Iman, has given me great comfort. I would like to express my heartfelt thanks to my late parents whose prayers and support will always be inscribed on my heart. I am also grateful to wonderful friends and colleagues who have

helped and supported me along the way, and who have made my stay in Penang enjoyable and meaningful. Thanks to all of you.

Finally, I would like to acknowledge the great support and patience of my small family (my wife, Dr. Lamia A. Al-Ta'ie, and my kids) who has shared both the joys and frustrations that the work has entailed. Thank you from the depth of my heart.

Ghassan Ezzulddin Arif

## TABLE OF CONTENTS

	Page
ACKNOWLEDGMENTS	ii
TABLE OF CONTENTS	iv
LIST OF TABLES	ix
LIST OF FIGURES	xii
LIST OF FLOWCHARTS	xiv
LIST OF ABBREVIATIONS AND ACRONYMS	xv
ABSTRAK	xx
ABSTRACT	xxii
<b>Chapter 1: INTRODUCTION</b>	1
1.1 Preface	1
1.2 Basic Definitions	3
1.2.1 Hexagonal Semiconductors Structures	3
1.2.2 Ionicity Factor	7
1.2.3 Lattice Constant	9
1.2.4 Bulk Modulus	10
1.2.5 Energy Gap	12
1.3 Problem Statements	13
1.4 Objectives	14
1.5 Research Methodology	15

1.5.1 Density Functional Theory	17
1.5.2 Full Potential of Linearized Augmented Plane Wave	18
1.5.3 WIEN2k package	18
1.6 Thesis Organization	21
<b>Chapter 2: LITERATURE REVIEW</b>	<b>23</b>
2.1 Introduction	23
2.2 Ionicity Factor	23
2.3 Bulk Modulus	28
2.4 WIEN2k Package	30
2.5 Summary	33
<b>Chapter 3: MATHEMATICAL MODELING OF IONICITY FACTOR IN TERMS OF ENERGY GAP</b>	<b>34</b>
3.1 Overview	34
3.2 The Process of Constructing the Proposed Ionicity Factor Model	35
3.2.1 Problem formulation	35
3.2.1.1 Determination of energy gap using WIEN2k package	35
3.2.2 Mathematical modeling of ionicity factor	39
3.2.2.1 Differentiating equation (3.6)	40
3.2.3 Verification by using pressure	45
3.2.4 Mathematical model evaluation	47
3.3 Summary	51

<b>Chapter 4: MATHEMATICAL MODELING OF IONICITY FACTOR IN TERMS OF LATTICE CONSTANTS</b>	<b>53</b>
4.1 Overview	53
4.2 The Process of Constructing the Proposed Ionicity Factor Model	53
4.2.1 Problem formulation	53
4.2.1.1 Determination of lattice constants using WIEN2k package	54
4.2.2 Mathematical modeling of ionicity factor	56
4.2.2.1 Differentiating equation (4.2)	57
4.2.3 Mathematical model verification based on pressure	60
4.2.4 Mathematical model evaluation	61
4.3 Summary	64
<b>Chapter 5: MATHEMATICAL MODELING OF BULK MODULUS IN TERMS OF LATTICE CONSTANTS</b>	<b>66</b>
5.1 Overview	66
5.2. The Process of Constructing Bulk Modulus Model	66
5.2.1 Problem formulation	66
5.2.1.1 Determination of lattice constants using WIEN2k package	67
5.2.2 Mathematical modeling of bulk modulus	68
5.2.2.1 Differentiating equation (5.2)	70
5.2.3 Verification of the mathematical model based on pressure	73
5.2.4 Mathematical model evaluation	74



5.3 Summary	77
<b>Chapter 6: MATHEMATICAL MODELING OF BULK MODULUS IN TERMS OF ENERGY GAP</b>	78
6.1 Overview	78
6.2 The Process of Constructing the Bulk Modulus Model	78
6.2.1 Problem formulation	79
6.2.1.1 Determination of energy gap using WIEN2k package	79
6.2.2 Mathematical modeling of bulk modulus	80
6.2.2.1 Differentiating equation (6.1)	82
6.2.3 Verification of the bulk modulus under pressure	85
6.2.4 Mathematical model evaluation	86
6.3 Summary	89
<b>Chapter 7: CONCLUSIONS AND FUTURE WORK</b>	91
7.1 Conclusions	91
7.2 Future Work	94
<b>REFERENCES</b>	95
<b>APPENDICES</b>	
<b>APPENDIX 1</b>	105
A.1.1 Input <i>ZnO</i> in Wurtzite Structures	107
A.1.2 Input <i>CdO</i> in Rock-Salt Structures	110
A.1.3 Determining <i>c/a</i> for <i>ZnO</i> in Wurtzite Structures	113

A.1.4 Determining $c/a$ for $CdO$ in Rock-Salt Structures	114
A.1.5 Determining $E_g$ for $ZnO$ in Wurtzite Structures	115
A.1.6 Determining $E_g$ for $CdO$ in Rock-salt Structures	120
<b>APPENDIX 2</b>	125
A.2.1 The Attempts of the Derivation of Ionicity Factor Model in Terms of Energy Gap	125
A.2.2 The Attempts of the Derivation of Ionicity Factor Model in Terms of Lattice Constants	128
A.2.3 The Attempts of the Derivation of Ionicity Factor Model in Terms of Lattice Constants	130
A.2.4 The Attempts of the Derivation of Bulk Modulus Model in Terms of Energy Gap	132
<b>APPENDIX 3</b>	135
Published Works by the Author Incorporated into the Thesis	141

## LIST OF TABLES

Table 1.1	Types of Structures	4
Table 3.1	Comparison of the Results of Ionicity Factor $f_{i1}$ and $f_{i2}$ in Terms of $E_g$ with Other References	43
Table 3.2	Determining Ionicity Factor at $P = 0$ (Atmospheric Pressure) and at the Critical Transition Pressure with Determining Energy Gap Corresponds to Pressure of Transition	46
Table 3.3	Comparison of the Percentage Error of $f_{i1}$ and $f_{i2}$ in Terms of $E_g$ with Experimental Values	48
Table 4.1	Comparing results between $f_{i1}$ and $f_{i2}$ with experimental and theoretical results	59
Table 4.2	Determined Ionicity Factor at $P = 0$ (Atmospheric pressure) and at the Critical Transition Pressure with Determining Lattice Constants Correspond to Pressure of Transition	61
Table 4.3	Comparison of the Percentage Error of $f_{i1}$ and $f_{i2}$ in Terms of $c/a$ with Experimental Values	63
Table 5.1	Determining $B_{o1}$ and $B_{o2}$ and Comparing Them with Experimental and Theoretical Values	72
Table 5.2	Determined Bulk Modulus at $P = 0$ and at the Critical Transition Pressure with Determining Lattice Constants Correspond to Pressure of Transition	74
Table 5.3	Comparison of the Percentage Error of $B_{o1}$ and $B_{o2}$ in Terms of $c/a$ with Experimental Values	75

Table 6.1	Comparison of the Results of Bulk Modulus $B_{o1}$ and $B_{o2}$ in Terms of $E_g$ with Other References	84
Table 6.2	Determined Bulk Modulus at $P = 0$ and at the Critical Transition Pressure with Determining Energy Gap Corresponds to Pressure of Transition	86
Table 6.3	Comparison of the Percentage Error of $B_{o1}$ and $B_{o2}$ in Terms of $E_g$ with Experimental Values	87
Table A.2.1	The Determinations of Attempts for Derivation the Ionicity Factor Model in Terms of Energy Gap for Hexagonal Structure Semiconductors	126
Table A.2.2	The Determinations of Attempts for Derivation the Ionicity Factor Model in Terms of Lattice Constants	129
Table A.2.3	The Determinations of Attempts for Derivation the Bulk Modulus Model in Terms of Lattice Constants	131
Table A.2.4	The Determinations of Attempts for Derivation the Bulk Modulus Model in Terms of Energy Gap	133
Table A.3.1	The Initial Values of Energy Gap $(E_g)_0$ and Ionicity Factor $(f_i)_0$ for Determining Differential Equations for Hexagonal Structure Semiconductors	135
Table A.3.2	The Initial Values of Lattice Constants $(c/a)_0$ and Ionicity Factor $(f_i)_0$ for Determining Differential Equations for Hexagonal Structure Semiconductors	137
Table A.3.3	The Initial Values of Lattice Constants $(c/a)_0$ and Bulk Modulus $(B_o)_0$ for Determining Differential Equations for Hexagonal Structure Semiconductors	138

Table A.3.4	The Initial Values of Energy Gap $(E_g)_0$ and Bulk Modulus $(B_o)_0$ for Determining Differential Equations for Hexagonal Structure Semiconductors	139
Table A.3.5	Periodic Table of Elements	140

## LIST OF FIGURES

Figure 1.1	Hexagonal unit cells with lengths $a, b, c$ and angles $\alpha, \beta, \gamma$ (Grosso & Parravicini, 2003).	4
Figure 1.2	Energy band levels for conductor, semiconductors, and an insulator (Grundmann, 2010).	5
Figure 1.3	Hexagonal structure of $NaCl$ (Reichardt & Welton, 2011).	8
Figure 1.4	Electrons distribution of $NaCl$ (Reichardt & Welton, 2011).	8
Figure 1.5	Illustration of uniform compression (Blakemore, 1985).	12
Figure 1.6	Allowed and forbidden ranges of energy for electrons in a crystal (Philips, 1973).	13
Figure 2.1	WIEN2k is used worldwide by about 2200 groups (Schwarz, 2014).	32
Figure 3.1	(a) Rock-Salt structure and (b) Wurtzite structure (m: Symmetry plane) (Grosso & Parravicini, 2003).	34
Figure 3.3	Values of the energy gap for Wurtzite semiconductor structures.	39
Figure 3.4	Behavior of the Equation (3.6) for different groups, for instance group IV-IV ( $\lambda_I = 0.23$ ), group III-V ( $\lambda_I = 0.65$ ) and other groups ( $\lambda_I = 1$ ).	40
Figure 3.5	Comparison between the obtained results of determining $f_{i1}$ and $f_{i2}$ in terms of energy gap with experimental results.	50
Figure 4.1	Total energy fitting of $CdS$ .	55
Figure 4.2	Total energy fitting of $SiC$ .	55
Figure 4.3	Behavior of the Equation (4.2) for different $\lambda_2 = 1, 2, 0.37$ for group III-V, I-VII, IV-IV, respectively and $\lambda_2 = 1.45$ for other groups.	57
Figure 4.4	Comparison between the obtained results of determining $f_{i1}$ and $f_{i2}$	64

in terms of lattice constants with experimental results.

Figure 5.1	Total energy fitting of <i>SiC</i> .	67
Figure 5.2	Total energy fitting of <i>CuCl</i> .	68
Figure 5.3	Behavior of the Equation (5.2) for some samples of $\lambda_3$ is equal to 0.665 for the group III-V, 0.886 for group IV-IV, 0.195 for group II-VI and 0.16 for groups	69
Figure 5.4	Comparison between the obtained results of determining $B_{o1}$ and $B_{o2}$ in terms of lattice constants with experimental results.	76
Figure 6.1	Values of the energy gap for rock-salt semiconductor structures.	79
Figure 6.2	Behavior of the Equation (6.1) for $\lambda_4 = 0.19$ , $\lambda_4 = 0.56$ , $\lambda_4 = 1$ , $\lambda_4 = 2.389$ , $\lambda_4 = 3.642$ , and $\lambda_4 = 0.56$ .	81
Figure 6.3	Comparison between the obtained results of determining $B_{o1}$ and $B_{o2}$ in terms of energy gap with experimental and theoretical results.	89

## LIST OF FLOWCHARTS

Flowchart 1.1	Research Methodology	20
Flowchart 3.2	Flow chart for the $n^{\text{th}}$ iteration in the self-consistent procedure (Reshak, 2013).	37



## LIST OF ABBREVIATIONS AND ACRONYMS

### *Abbreviation*

<i>BZ</i>	Brillouin Zone
CP	Critical point
DOS	Density of states
1D	One-dimensional
2D	Two-dimensional
3D	Three-dimensional
<i>eV</i>	Electron-volt, $1 \text{ eV} = 1.602189 \cdot 10^{-19} \text{ Joule}$
<i>V</i>	Volt
<i>D</i>	Distance
<i>dA</i>	Differential area
<i>E</i>	Energy
<i>E<sub>g</sub></i>	Energy gap
VB	Valence-Band
<i>f<sub>i</sub></i>	Ionicity
<i>t</i>	Time
T	Temperature [C°]
°	Degree
<i>P</i>	Pressure
P	Density [kg/m <sup>3</sup> ]

### ***Abbreviation***

$O$	Reflection coefficient (dimensionless)
$P_t$	Transition pressure
$\Gamma$	The maximum of the valence-band ( $VB$ ) for most semiconductors is at the $\Gamma$ point
Hz	Hertz
II-VI	Group II, group VI of periodic table
DE	Differential equation
$B_o$	Bulk modulus
$c/a$	Lattice constants
FP-LAPW	Full potential of linearized augmented plane wave
DFT	Density functional theory
EV-GGA	Engel Vosko-General Gradient Approximation
$RS$	Rock-Salt
$ZB$	Zinc-Blende
$W$	Wurtzite
a.u.	Atomic units
$\text{\AA}$	$1 \text{\AA} = 10^{-8} \text{ cm} = 10^{-10} \text{ m}$ (order of magnitude of the atomic dimensions)  Unit cell parameters (in a.u., $1 \text{ a.u.} = 0.529177 \text{\AA}$ ).
Bohr	$1 \text{ Bohr} = 0.529177208 \text{\AA}$
$\text{eV}/\text{\AA}^3$	$1 \text{ eV}/\text{\AA}^3 = 160.2176487 \text{ GPa}$

### ***Abbreviation***

GPa	Giga Pascal = $10^4$ bars
Mbar	1 Mbar = 100 GPa
Kbar	1 kbar = 1000 bar
Atm	1 atm = 1.01325 bar = 0.000101325 GPa
Pascal	1 pascal = 1.0E-09 GPa
$R_{MT}$	The average radius of the muffin-tin spheres
$K_{max}$	The maximum value of the wave vector
$\alpha, \beta, \gamma$	Crystal angles
MULT	Number of equivalent atoms of this kind
ISPLIT	An output-option for WIEN2K package.
NPT	Number of radials meshes points
R0	First radial mesh point (typically between 0.0005 and 0.00005)
RELA	Fully relativistic core and scalar relativistic valence
RMT	Muffin-tin radius
$E(\bar{r})$	Internal energy
$E_v$	The top of the valence band
$E_c$	The bottom of the conduction band

**Table.** Names of Compounds

<b>No.</b>	<b>Compound</b>	<b>Name of Compound</b>	<b>Group</b>
1	AgF	Silver Fluoride	II-VII
2	AgCl	Silver Chloride	II-VII
3	AgBr	Silver Bromide	II-VII
4	AgI	Silver Iodide	II-VII
5	CaO	Calcium Oxide	II-VI
6	CdO	Cadmium Oxide	II-VI
7	CuCl	Copper Chloride	II-VII
8	CaS	Calcium Sulfide	II-VI
9	CuBr	Copper Bromide	II-VI
10	CdSe	Cadmium Selenide	II-VI
11	CaTe	Calcium Telluride	II-VI
12	MgS	Magnesium Sulfide	II-VI
13	MgO	Magnesium Oxide	II-VI
14	SrO	Strontium Oxide	II-VI
15	SrS	Strontium Sulfide	II-VI
16	ZnO	Zinc Oxide	II-VI
17	ZnS	Zinc Sulfide	II-VI
18	ZnSe	Zinc Selenide	II-VI
19	AlN	Aluminum Nitride	III-V
20	GaN	Gallium Nitride	III-V
21	InN	Indium Nitride	III-V
22	KF	Potassium Fluoride	I-VII
23	KBr	Potassium Bromide	I-VII
24	KCl	Potassium Chloride	I-VII
25	KI	Potassium Iodide	I-VII
26	LiF	Lithium Fluoride	I-VII
27	LiCl	Lithium Chloride	I-VII
28	LiBr	Lithium Bromide	I-VII

<b>No.</b>	<b>Compound</b>	<b>Name of Compound</b>	<b>Group</b>
29	LiI	Lithium Iodide	I-VII
30	NaF	Sodium Fluoride	I-VII
31	NaCl	Sodium Chloride	I-VII
32	NaBr	Sodium Chloride	I-VII
33	NaI	Sodium Iodide	I-VII
34	RbF	Rubidium Fluoride	I-VII
35	SiC	Silicon Carbide	IV-IV
36	CdS	Cadmium Sulfide	II-VI
37	MgTe	Magnesium Telluride	II-VI
38	MgSe	Magnesium Selenide	II-VI
39	BeO	Beryllium Oxide	II-VI

Note. All elements are mentioned in the periodic Table A.3.5 in Appendix 3.

# **PEMODELAN MATEMATIK BAGI FAKTOR KEIONAN DAN MODULUS PUKAL UNTUK BAHAN SEMIKONDUKTOR HEKSAGON PENDUAAN**

## **ABSTRAK**

Bahan semikonduktor telah menjadi penting dan utama dalam pembuatan beberapa perkakasan elektronik. Medium elektronik terkini telah menyaksikan bahan semikonduktor termaju diperlukan untuk menambahbaik keupayaan sesuatu bahan elektronik. Disebabkan kepelbagaian aplikasi dalam teknologi perkakasan elektronik, struktur semikonduktor itu perlu dikaji sifatnya. Dalam tesis ini, semikonduktor bersifat heksagon penduaan akan dikaji melibatkan struktur dan sifat keelektrikannya terhadap faktor keionan serta modulus pukal. Struktur garam batu (Rock Salt) dan wurzit (Wurzite) akan dijadikan fokus kajian kerana ia merupakan bahan utama bagi semikonduktor heksagon penduaan. Fokus kajian tertumpu kepada penentuan sifat keionan dan modulus pukal bahan-bahan ini melalui pembinaan model-model matematik berkaitan. Pembinaan model matematik berdasarkan faktor keionan dan modulus pukal adalah dalam sebutan jurang tenaga ( $E_g$ ) serta pemalar kekisi ( $c/a$ ) bagi bahan garam batu dan wurzit tersebut. Pembinaan model ini berdasarkan Teori Fungsian Ketumpatan dari Gelombang Satah Imbuhan Potensi Penuh dan Penghampiran Kecerunan Umum Engel Vosko dengan menggunakan pengaturcaraan WIEN2k. Pengesahan model yang dibina adalah berdasarkan perbandingan dengan data eksperimen dari beberapa kajian penyelidikan terdahulu dalam kondisi berbeza seperti pengesahan berdasarkan tekanan. Ditunjukkan dalam tesis ini melalui ilustrasi taburan dan gambarajah bahawa keputusan bagi model yang dibina adalah seiring dengan data eksperimen penyelidikan tersebut. Keputusan daripada kajian ini adalah lebih jelas dan

berupaya menjadi alat matematik dalam menyelesaikan masalah melibatkan faktor keionan serta modulus pukal bagi struktur garam batu dan wurzit.

# **MATHEMATICAL MODELLING OF IONICITY FACTOR AND BULK MODULUS FOR HEXAGONAL BINARY SEMICONDUCTOR MATERIALS**

## **ABSTRACT**

Semiconductor materials have become important as being the main ingredients in almost all electronic devices. The current electronic medium has seen that advanced semiconductor materials are needed to enhance the capability of electronic materials. Due to their numerous applications in technology and electronic devices, hexagonal binary semiconductor structures will be explored in this thesis and their structural and electrical properties for ionicity factor and bulk modulus will be investigated as well. Rock Salt and Wurtzite structures will be considered in this thesis since these structures are considered as a major part of the hexagonal binary semiconductors. The aim of this thesis is to find exact determinations of ionicity factor and bulk modulus in terms of energy gap ( $E_g$ ) and lattice constants ( $c/a$ ) for Rock Salt and Wurtzite structures. These determinations are conducted by using Density Functional Theory (DFT) of Full-Potential Linear Augmented Plane Wave (FP-LAPW) which is a method constructed by utilizing the WIEN2k programming code within Engel Vosko-General Gradient Approximation (EV-GGA). The validation of the constructed models is done by comparing them with different researchers' experimental data under different conditions such as exposing these mathematical models to pressure. It has been shown from illustrated tables and figures that the models results are well conformed to experimental values of other researchers. The results of the present study are very straightforward and able to become mathematical tool for solving physical problems involving ionicity factor and bulk modulus with respect to Rock Salt and Wurtzite structures.



# CHAPTER 1

## INTRODUCTION

### 1.1 Preface

A semiconductor is a material with small but nonzero energy gap which behaves as an insulator at absolute zero, but allows thermal excitation of electrons into its conduction band at temperatures below its melting point. It is materials that are among the properties of a conductor and an insulator. A semiconductor is commonly used and found in almost all electronic devices. Examples of semiconductor materials are germanium, selenium, and silicon. Semiconductor materials constitute the basic building blocks of emitters and receivers in cellular, satellite, liquid-crystal-display televisions (LCD-TV), and fiberglass communication. The semiconductors have largely replaced vacuum tubes in electronics, allowing for more complex and smaller electronic devices and modern computers. Therefore, because of their numerous applications in technology and electronic devices, they have been subjects of many researchers and the main subject of the present thesis as well.

Binary semiconductor structures are chemical compounds that contain exactly two different elements, e.g. *SiC*, *GaAs*, *Cds*. Studies of electronic and structural properties of binary semiconductors have received considerable attention, both experimentally and theoretically (Gurunathan *et al.*, 1999). Ionicity factor and bulk modulus are among these properties which have been determined since the invention of semiconductors in the mid of the 20th century.

The hexagonal binary semiconductor structures have high melting point, high thermal conductivity and large bulk modulus. These properties as well as wide energy gaps are closely related to strong bonding. Due to this, the electronic and structural properties of ionicity factor and bulk modulus for Wurtzite and Rock-Salt structures that constitute major part of the hexagonal binary semiconductors are determined.

The electronic and structural properties of the hexagonal binary semiconductor materials have been investigated by various researchers such as Phillips (1970, 1973), Harrison (1973), Pauling (1932, 1939, 1960), García and Cohen (1993), Wang and Ye (2002) and others. However, in spite of much research on the fundamental properties and device applications of the hexagonal semiconductor structures, the ionicity factor, and bulk modulus, in terms of energy gap and lattice constants, for the Wurtzite and Rock-Salt hexagonal semiconductor structures have not been given full attention. This motivated us to conduct a study for determining the electronic and structural properties of the hexagonal phase for Wurtzite and Rock-Salt structures by constructing mathematical models.

Mathematical approaches are used in the mathematical modeling for finding solutions to ionicity factor and bulk modulus with respect to Wurtzite and Rock-Salt structures.

In this study, ionicity factor and bulk modulus of Wurtzite and Rock-Salt structures have been determined by constructing four mathematical models and several results have been obtained by comparing it to an experimental data. The proposed mathematical models in this study can assist physicists in finding the determinations of

ionicity factor and bulk modulus for Wurtzite and Rock-Salt of hexagonal binary semiconductor structures.

## **1.2 Basic Definitions**

This section gives basic definitions of the physical terms used throughout this thesis. The terms which will be discussed are hexagonal semiconductors structure, ionicity factor, bulk modulus, lattice constants and energy gap.

### **1.2.1 Hexagonal semiconductor structures**

A semiconductor is a material that is neither metals nor insulators. Such material has electrical conductivity between conductor such as copper and an insulator such as glass. Consequently, the electrical properties of the semiconductors are intermediate between metals and insulators. This is due to the special arrangement of energy level electrons in semiconductors (Phillips, 1971). The crystal structures contain a collection of atoms that are closely packed into the shape of a hexagon. The hexagon is then characterized by the existence of a single six symmetry axis. The structure of hexagonal semiconductors consists of three lattice constants and three angles between them, shown in Figure 1.1. Parameter  $a$ ,  $b$ ,  $c$  refers to the sides of the hexagon, in which  $a = b$ ,  $b \neq c$ ,  $\alpha = \beta = 90^\circ$ ,  $\gamma = 120^\circ$  (Grosso & Parravicini, 2003).

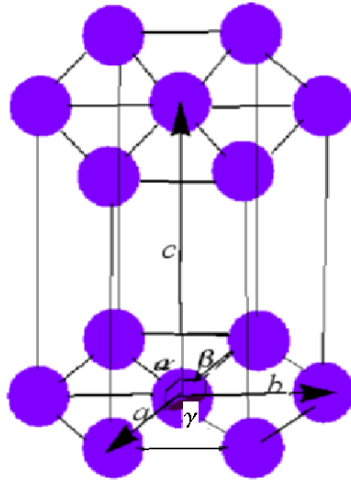


**Figure 1.1.** Hexagonal unit cells with lengths  $a$ ,  $b$ ,  $c$  and angles  $\alpha$ ,  $\beta$ ,  $\gamma$  (Grosso & Parravicini, 2003).

Other structures such as monoclinic, trigonal, tetragonal, orthorhombic and cubic are different from hexagonal structures in term of relationship between the sides of the structures and the relationship between the angles of the structures as shown in Table 1.1.

**Table 1.1** Types of Structures

Type	Conditions
Monoclinic	$a \neq b \neq c, \alpha = \beta = 90^\circ \neq \gamma$
Trigonal	$a = b = c, \alpha = \beta = \gamma < 120^\circ \neq 90^\circ$
Tetragonal	$a = b \neq c, \alpha = \beta = \gamma = 90^\circ$
Orthorhombic	$a \neq b \neq c, \alpha = \beta = \gamma = 90^\circ$
Cubic	$a = b = c, \alpha = \beta = \gamma = 90^\circ$
Hexagonal	$a = b \neq c, \alpha = \beta = 90^\circ, \gamma = 120^\circ$

There are many types of hexagonal binary semiconductor structures such as Wurtzite, Rock-Salt, Zinc-Blende, Chalcopyrite, Fluorite, Delafossite, Perovskite, and etc. (Grundmann, 2010). The Wurtzite mineral is a crystal structure of various binary compounds. It is an example of the hexagonal crystal system. Rock-Salt is a chemical compound belonging to the larger class of ionic salts; salt in its natural form is crystalline mineral and known as Rock-Salt or Halite.

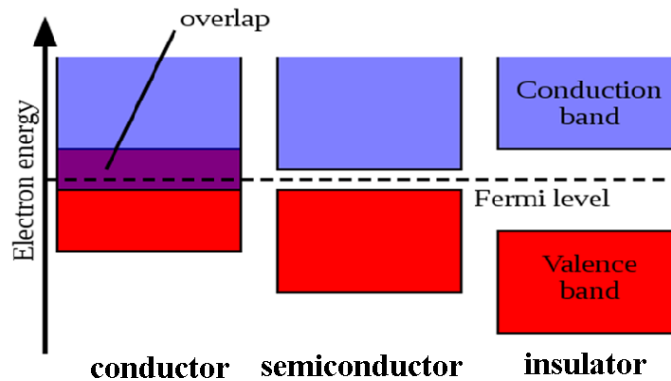


**Figure 1.2.** Energy band levels for conductor, semiconductors, and an insulator (Grundmann, 2010).

Figure 1.2 illustrates the energy band level for insulators, semiconductors and conductors, and reflects three levels of bands; valence band, energy gap which contains Fermi level and conduction bands. The Fermi level is defined as total chemical potential for electrons or is known as electrochemical potential for electrons, and can be referred to  $E_F$ . The valence band is the highest range of electron energies in which electrons are normally present at an absolute zero temperature. The valence band is located below the conduction band separated from it in insulators and semiconductors by an energy gap. The energy gap is the separation of energy between highest valence

band state and the lowest conduction band state. In metals, the conduction band has no energy gap to separate it from the valence band. The conduction band quantifies the range of energy required to free an electron from its bond to an atom. In general, various materials can be classified by their energy gap which can be defined as the difference between the valence and conduction bands.

Unlike insulators, which work qualitatively through classical ionic models, the semiconductors display predominantly covalent structures that have challenged the understanding both chemists and physicists. A covalent bond is a chemical bond that involves sharing of electron pairs between atoms. In conductors, the valence and conduction bands may overlap, so they may not have an energy gap. However, semiconductors' substance can act as an electrical conductor or insulator depending on chemical alterations or external conditions. In addition, the conductivity of a semiconductor increases as temperature increases (Adachi, 2009).

It is important to note that all solids have a characteristic of their energy band structure. Variation in band structure is responsible for the wide range of electrical characteristics observed in various materials (John *et al.*, 2010). The invention of the transistor in 1948 had stimulated great interest in the energy bands of semiconductors and by the middle fifties, this topic had become quite fashionable (Phillips, 1971).

Semiconductors and insulators have electrons that refer to the number of energy gap denoted by  $E_g$ . The maximum of the valence band for most semiconductors is at  $\Gamma$  point where  $\Gamma$  is a center of the Brillouin zone (*BZ*) with (0,0,0) coordination (Wang & Ye, 2002). However, the electron can jump and transit from a valence band to a

conduction band relying on a specific minimum amount of energy. Electrons can get enough energy to jump to the conduction band by absorbing either a temperature or a light rays. The energy gap typically decreases with increasing temperature.

### 1.2.2 Ionicity factor

The ionicity factor of a bond can be defined as the fraction of ionic denoted by  $f_i^\alpha$  or heteropolar character. Heteropolar is an energy gap for two or more elements. For instance Zinc-Blende, Wurtzite, and Rock-Salt in the bond are compared with the fraction of covalent  $f_h^\alpha$  or homopolar character. Homopolar is an energy gap for Diamond structures such as *Si* and *Ge*. By definition, these fractions satisfy the relation (Adachi, 2009).

$$f_i^\alpha + f_h^\alpha = 1, \quad (1.1)$$

where  $\alpha$  is referring to electronic polarizability. The ionic materials are bound solely by the balance of electrostatic forces and can be described as an array of spherical ions in a simple structure such as Rock-Salt (Rez & Muller, 2008). However, the heteropolar or ionic bond is the consequence of the electrostatic attraction between the ions (Grundmann, 2010). The focus in this thesis is on heteropolar character of Wurtzite and Rock-Salt hexagonal binary structures.

Crystals, such as sodium chloride (*NaCl*) which is combination of  $Na^+$  and  $Cl^-$ , have ionicity factor constituting from positively and negatively charged ions. In *NaCl* ionic bonding, electrons are moving from low electronegative atom, which becomes a positive ion to high electronegative atom, which is then transformed into a negative ion (refer to Figure 1.3 and Figure 1.4).

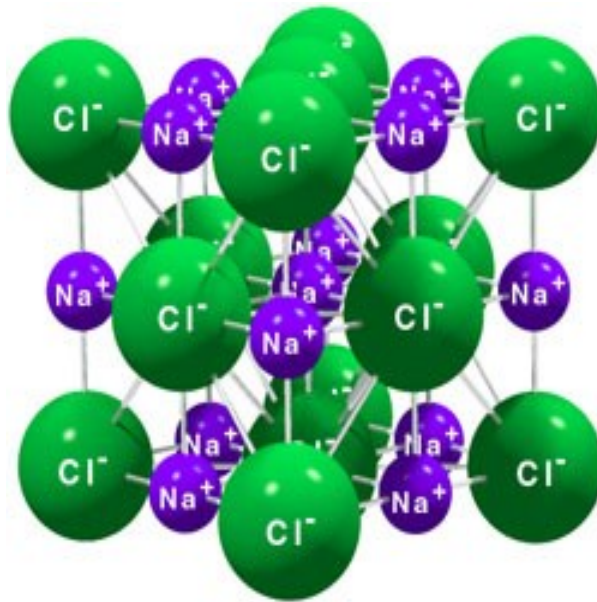


**Figure 1.3.** Hexagonal structure of  $NaCl$  (Reichardt & Welton, 2011).

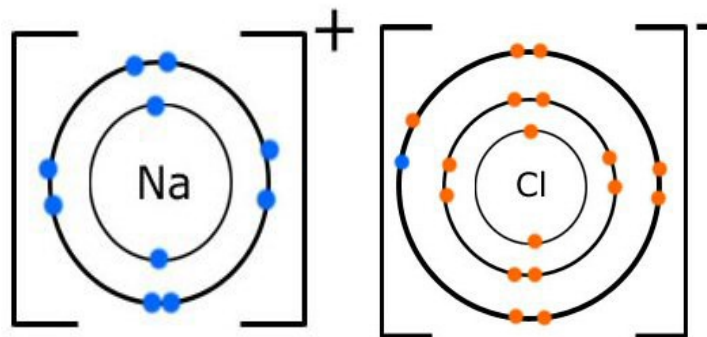


**Figure 1.4.** Electrons distribution of  $NaCl$  (Reichardt & Welton, 2011).

In general, ionicity factor is useful for describing the qualitative chemical behavior of elements, but very difficult to define the quantitative elements (Phillips, 1970). It measures the ability of an atom or molecule to attract electrons in the context of a chemical bond. In  $NaCl$ , the ionization energy denoted by  $E_i$  is an energy required to move an electron from a neutral isolated atom to an ion with a positive charge;  $Na +$



$E_i \rightarrow Na^+ + e^-$ , where  $Na$  has 5.14 eV (electron volt). On the other hand,  $E_a$  is the energy required to move an electron to an ion with a negative charge;  $Cl + e^- \rightarrow Cl^- + E_a$  where  $Cl$  has 3.56 eV (Reichardt & Welton, 2011).

### 1.2.3 Lattice constant

Lattice constant is a parameter referring to constant distance between unit cells in a crystal lattice. Full set of lattice parameters consists of the three lattice constants and the three angles between them. The three dimensions lattices have three lattice constants, which refer to  $a$ ,  $b$ , and  $c$  (see Figure 1.1). However, for hexagonal crystal structures, the lattice can be defined by only two length parameters,  $a$  and  $c$ , as  $a = b$ . Since in cubic structures the lattice  $a = b = c$ , the cubic structures have only one length parameter,  $a$ . In addition, there is significant structural difference between bond distance in Rock-Salt and Wurtzite structures. The Rock-Salt structure has only one type of second-neighbor cation–anion bond distance (six bonds in cubic structure only) (Ambacher *et al.*, 2002; Adachi, 2009):

$$d(A-B) = \frac{a}{2}, \quad (1.2)$$

where  $d$  is a distance between  $A$  anion and  $B$  cation and  $a$  is the length of the lattice constant. The numbers of bonds depend on the chemical reaction and the type of neighbor cation–anion.

Furthermore, Wurtzite structure has two types of first-neighbor cation–anion bond distances; along  $a$ -axis (one bond in cubic structure) (Ambacher, 2002; Adachi, 2009):

$$d(A-B) = ua, \quad (1.3)$$

and in the basal plane (three bonds in hexagonal structure) (Ambacher, 2002; Adachi, 2009):

$$d(A-B) = \sqrt{\frac{1}{3} + \left(\frac{1}{2} - u\right)^2 \left(\frac{c}{a}\right)^2} a, \quad (1.4)$$

Here,  $u$  represents cell internal structural parameter. The interatomic distance for the basic unit is described by internal parameter  $u$ . The ideal Wurtzite parameters are given by  $c/a = (8/3)^{1/2} \approx 1.633$  and  $u = 3/8$ .

Note that lattice constants can be affected by temperature and pressure. The temperature dependence on lattice constants is explained by thermal expansion coefficient (Adachi, 2009).

#### 1.2.4 Bulk modulus

Bulk modulus, refers to  $B_o$  is the hardness parameter linked with structural parameter that has a cell volume. Hardness parameter shows a systematic reduction with the increase in cell volume. It is essential to mention that the bulk modulus and cohesive energy are important ground state properties of a material. Both experimental and theoretical results suggested that the bulk modulus reflects the hardness of the materials (Singh *et al.*, 2009).

Recently, bulk modulus of semiconductors has become physical interest and practical importance interpretation of high-pressure experimental data (Milman *et al.*, 2000). Bulk modulus defines its resistance to volume change when material is compressed. Thus, bulk modulus of semiconductors measures the resistance of the semiconductors to uniform pressure. In this case, the bulk modulus is being defined as the ratio of pressure increase to the resulting relative decrease of the volume. Generally, the bulk modulus always greater than zero and can be defined by Cohen (1985):

$$B_o = \frac{-VdP}{dV}. \quad (1.5)$$

The negative sign on the right part of the Equation (1.5) is referring to an attractive force between electron and nucleus,  $P$  and  $V$  are the pressure and volume and  $dP/dV$  is the derivative of pressure with respect to volume. The bulk modulus at zero temperature is given by

$$B_o = \frac{\rho dP}{d\rho}, \quad (1.6)$$

where  $\rho$  refers to density in  $\text{kg/m}^3$  and  $dP/d\rho$  is derivative of pressure with respect to density. For solids such as alkali-halide crystals, the reasonable estimates of the bulk modulus can be written as

$$B_o = \frac{-VdP}{dV} = \frac{Vd^2E}{dV^2}, \quad (1.7)$$

where  $E$  is energy. The experimental measurements of bulk modulus are utilized to fix the parameters of specific models (Cohen, 1985).

Figure 1.5 shows uniform compression for a material, where volume decreases with the increase in pressure.

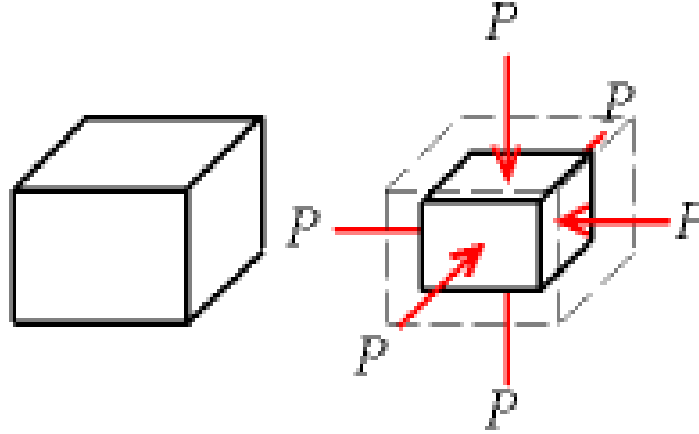


**Figure 1.5.** Illustration of uniform compression (Blakemore, 1985).

### 1.2.5 Energy gap

Energy gap or band gap denoted by  $E_g$  is an energy range of solid material where no electron states can exist. Generally in a solid state physics, the energy gap of electronic band structure denotes the energy difference between bonding and anti-bonding levels. The energy difference is denoted by  $\Delta E_{cv}$  between  $E_v$ , the top of the valence band, and  $E_c$ , the bottom of the conduction band.  $E_{cv}$  determines the electrical properties of the semiconductor, and energy gap that most influences structural properties, energy gap can be written as

$$E_g = \bar{E}_c - \bar{E}_v, \quad (1.8)$$

where  $\bar{E}_c$ ,  $\bar{E}_v$  are average of the conduction and valence band energies respectively.

Figure 1.6 displays the ranges of energy for electrons in a crystal, where  $E_v > \bar{E}_v$ ,  $E_c < \bar{E}_c$  and  $\Delta E_{cv} < E_g$ . The term  $\rho(E)$  is a nonzero density of electronic band states, and  $N(E)$  is the number of electronic states per unit volume. It also shows the valence and

conduction bands and the energy gap between them ( $\Delta E_{cv}$ ) as well as the average gap (Philips, 1973).

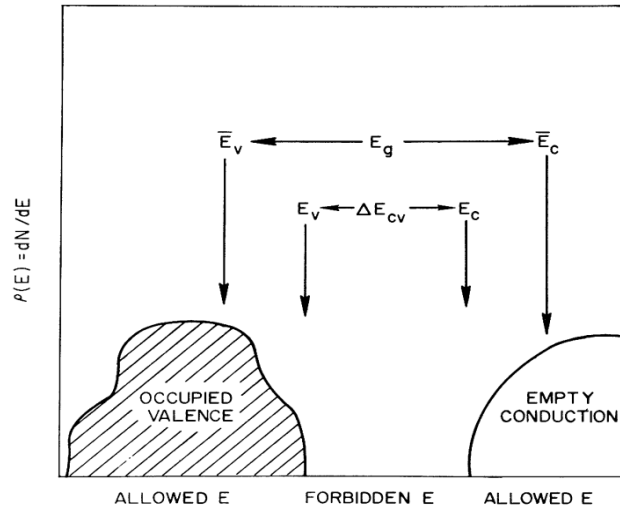


**Figure 1.6.** Allowed and forbidden ranges of energy for electrons in a crystal (Philips, 1973).

The conductivity of semiconductors is strongly dependent on the energy gap. The only available carriers for conduction are through electrons which have enough thermal energy to excite across the energy gap. Thus, the energy gap is considered a major factor in determining the electrical conductivity of semiconductors. It is also important to note that the energy gap of semiconductors tends to decrease as the temperature is increased.

### 1.3 Problem Statements

Since there have been few studies done particularly in investigating and solving the physical problems of ionicity factor and bulk modulus based on energy gap and lattice constants, the rationale of this research is to solve these physical problems by considering electronic and structural properties of the hexagonal binary structures of

semiconductors. Although there are different types of semiconductors like ternary and quaternary structures suitable for different applications, the current study focuses on binary structures as they are considered the basis for different materials and widely used by physicists. The study depends on the mathematical modeling to express ionicity factor and bulk modulus.

#### **1.4 Objectives**

The main objectives of this study are:

- ❖ To find a proper mathematical model that helps in determining the ionicity factor and bulk modulus for hexagonal binary semiconductors, focusing on Wurtzite and Rock-Salt structures
- ❖ To choose mathematical equations which lead to construction of new mathematical models.
- ❖ To determine energy gap and lattice constants through WIEN2K package to be used as input data that helps in the process of constructing the proposed models.
- ❖ To determine the ionicity factor and bulk modulus in terms of energy gap and lattice constants for Wurtzite and Rock-Salt structures conducted through the proposed model.
- ❖ To compare the results obtained from the proposed model of ionicity factor and bulk modulus with previous literatures.
- ❖ To verify the constructed mathematical model by addressing the errors and to minimize such errors.

## 1.5 Research Methodology

In the light of research methodology, it is important to distinguish two methods used in the construction of the proposed mathematical models. The first method includes certain guidelines and typical steps as following:

- 1- Problem formulation: Formulating the problem by explaining the main objectives of the proposed mathematical model and by choosing the variables and parameters that constitute the mathematical equation of the proposed model (Bender, 1978). This step also involves the determination of energy gap and lattice constants using WIEN2k package before constructing the mathematical models of ionicity factor and bulk modulus.
- 2- Mathematical model building: This step involves connecting the relationships among the variables and interpreting them mathematically to obtain a model for the phenomenon. Thus, the mathematical models are constructed by finding the equation to solve the physical problems represented through determining the ionicity factor and bulk modulus, in terms of the energy gap and lattice constants. This step also includes mathematical interpretation, i.e., applying appropriate mathematical analysis to the proposed model and at the same time differentiating the chosen equation.
- 3- Mathematical model verification: This step is regarded as an important part of the process of constructing the mathematical model as the verification tests are designed to address the errors discovered while applying the proposed model. This way helps minimize such errors and enhance the model. In addition, the verification test involves a comparison between the result obtained by the

proposed model and the experimental and theoretical values of other researchers. The verification of the proposed model against experimental data obtained should be done under different conditions such as temperature and pressure. When testing the validation of the constructed models, it is ensured that they can solve real physical problem, and the results obtained by the models were in reasonable agreement with the experimental and theoretical data.

- 4- Mathematical model evaluation: This step is concerned with evaluating the constructed model in the study. When evaluating the constructed models, it is found out that these models have minimum errors.

The last two steps are called experimental process that necessitates the acquisition of experimental data and exposing the proposed models to certain conditions like pressure and temperature. The experimental data allows establishing the accuracy and adequacy of the proposed model through the comparison between the experimental data and the results obtained from the constructed mathematical models. Once the model is built, it should work according to its rules of operation.

The second method includes main techniques that are used in conducting the determinations of the energy gap, and lattice constants as an input data for the modeling of ionicity factor and bulk modulus; The techniques are Density Functional Theory (DFT) (will be explained in Section 1.5.1), Full Potential of Linearized Augmented Plane Wave (FP-LAPW) with the WIEN2k package (will be explained in Section 1.5.2 and 1.5.3, respectively). The research methodology of this thesis is given in Flowchart 1.1.



### 1.5.1 Density functional theory

Density Functional Theory (DFT) was introduced by Kohn and Sham (1965) and becomes the most successful method to compute the electronic structure of a material. DFT has become the undisputed number-one *ab initio* (*ab initio* is different methods grouped into first-principle approaches that have been developed to compute the electronic structure of solids) theory for the computation of the electronic structures that are widely used in solid state physics and quantum chemistry as well as in bio-chemistry. The focus of the majority of solid state DFT calculations is often semiconductors, simple metals and transition metals, applying the Local Density Approximation (LDA) or Generalized-Gradient Approximation (GGA). For these materials, properties that are well described and determined by DFT include energy gap and lattice constants (Niesert, 2011).

By using DFT, many computed properties are in very good agreement with corresponding experiments, unveiling predictive power for properties that still have to be measured or even materials that have yet to be synthesized (Niesert, 2011). DFT is derived from the electron density and many-electron system properties which can be determined by using functional. Functional is a function of another function, which refers to the spatially dependent electron density. Many-electron wave function is denoted by  $\Psi(r_1\sigma_1, \dots, r_N\sigma_N)$  where  $r$  is radius of the atom,  $N$  is the number of electrons containing information needed and  $\sigma$  is conductivity. It is also a function of many variables, which is difficult to determine, store or apply (Bodnar, 2004).

In general, behaviors of electrons comprising of bond strength of the system will determine the properties of a material. In DFT, the ground state of an interaction of

electron gas is mapped onto the ground state of a non-interacting electron gas, which experiences an effective potential. This mapping is principle in research done by Ao and Jiang (2009) given exact ground-state properties (Ao & Jiang, 2009).

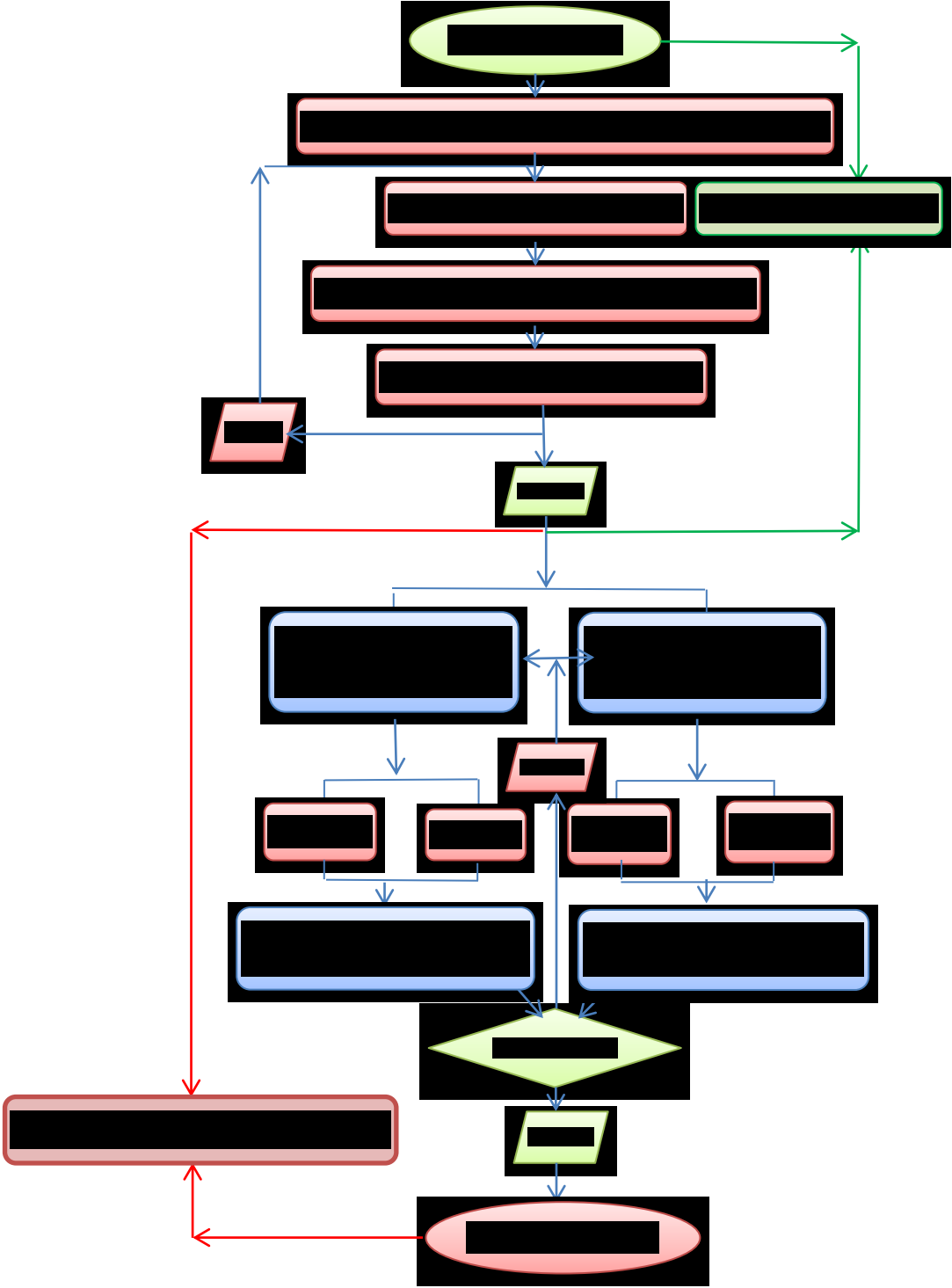
### **1.5.2 Full Potential of Linearized Augmented Plane Wave**

Full Potential of Linearized Augmented Plane Wave (FP-LAPW) is a method build using WIEN2k programing code (Blaha *et al.*, 2013). Linearized Augmented Plane Wave (LAPW) has proven to be an effective basis for the solution of the Kohn-Sham equations, which is the main calculation task for approximation of local spin density for DFT (Blaha *et al.*, 1990). A self-consistent scheme is solved via DFT using the Kohn-Sham equation (Kohn & Sham, 1965; Hohenberg, 1964). The determinations are based on the total-energy determinations using the FP-LAPW method. The exchange and correlation potential is treated by the Generalized Gradient Approximation (GGA) for total-energy calculations. Furthermore, the exchange correlation potential uses Engel Vosko-Generalized Gradient Approximation (EV-GGA) (Engel & Vosko, 1993) as valence electrons of total energy for electronic properties.

### **1.5.3 WIEN2k package**

WIEN2k is a programing code designed to utilize systematic file for controlling the program flow and passage of results. WIEN is introduced in 1990 (Blaha *et al.*, 1990), and is written in FORTRAN 90 which requires a UNIX (LINUX) operating system. It has been implemented successfully on the following computer systems: Pentium systems running under Linux, IBM RS6000, HP, SGI, Compac DEC Alpha, and SUN. It is expected to run on any modern UNIX system (Blaha *et al.*, 2013).

The input data needed for WIEN2k package are lattice constants ( $a = b$  and  $b \neq c$ ), angles ( $\alpha, \beta, \gamma$ ), space group, and atomic positions ( $x, y, z$ ). In hexagonal structures, the space group is 216 which includes 24 symmetry operations and excludes inversion symmetry. The Muffin-Tin (MT) radii were assumed to be 2.0 atomic units (*a.u.*) for each element. The dependence of the total energy on the number of  $k$  points in the irreducible wedge of the first ( $BZ$ ) (Phillips, 1973) has been explored within the linearized tetrahedron scheme (Blaha *et al.*, 2013) by performing the determination for 10  $k$  points. A satisfactory degree of convergence was achieved by considering a number of FP-LAPW basis functions up to  $R_{MT} K_{max} = 8$  ( $R_{MT}$  is the average radius of the MT spheres and  $K_{max}$  is the maximum value of the wave vector). The values of  $R_{MT}$  and  $K_{max}$  for a whole range of lattice spacing are retained. Flowchart 1.1 explains the research methodology used in this work.



**Flowchart 1.1.** Research Methodology.

## 1.6 Thesis Organization

This thesis is organized as follows:

Chapter 1 describes the background of hexagonal binary semiconductor structures and entails the problem statement, objectives, research methodology. The basic definitions of concepts and terms that will be called upon in the next chapters are introduced in this chapter.

Chapter 2 presents a literature review on ionicity factor and bulk modulus. It also introduces review of the most important studies of the WIEN2k package that is used to determine the input data utilized in constructing the proposed models in this study.

Chapter 3 discusses the typical steps that are used in the modeling of the mathematical model whose target is to determine the ionicity factor for hexagonal binary semiconductor structures. This chapter focuses on the determination of the energy gap by using WIEN2k code (Blaha *et al.*, 2013). The correlation between the ionicity factor and the electronic properties, energy gap of hexagonal binary semiconductor structures, is discussed. One of the main steps that are used in building the mathematical model is the verification process.

Chapter 4 investigates the process of the mathematical modeling that is followed in the construction of the proposed mathematical model, which will be constructed to determine the ionicity factor for the hexagonal binary semiconductor structures. This chapter investigates the determination lattice constants by using WIEN2k code (Blaha *et al.*, 2013). In this chapter, the correlation between the ionicity factor and the structural properties, lattice constants of hexagonal binary semiconductor structures, is

also presented. To ensure the accuracy and correctness of the ionicity factor model, it is verified under different conditions like pressure.

Chapter 5 addresses the typical steps and the guidelines that are used in the modeling of the mathematical model which aims to determine the bulk modulus for hexagonal binary semiconductor structures based on lattice constants. The lattice constant is determined by using WIEN2k code (Blaha *et al.*, 2013) to be prepared as an input data in constructing the proposed mathematical model. This chapter also describes the verification of the proposed model under certain condition such as pressure. The results of the verification are presented in this chapter.

Chapter 6 provides the process of the modeling of the mathematical model and choosing the differential equation, which leads to the construction of the model. The proposed mathematical model is built to determine the bulk modulus for hexagonal binary semiconductor structures based on energy gap. To prepare the input data that is used in constructing the model, the energy gap, is determined by using WIEN2k code (Blaha *et al.*, 2013). This chapter describes the verification of the proposed model under certain condition such as pressure. The result of the verification shows that there is an agreement between the resulted values obtained from the proposed mathematical model and experimental and theoretical data.

Chapter 7 summarizes the findings of the study and suggested areas for future research.

## CHAPTER 2

### LITERATURE REVIEW

#### 2.1 Introduction

This chapter gives a literature review related to ionicity factor and bulk modulus. Survey of significant studies conducted on ionicity factor is presented in Section 2.2. The important studies on bulk modulus are briefly discussed in Section 2.3. Section 2.4 introduces a review of the important studies using the WIEN2k package, which is used in this study to find the input data. Finally, a short summary is introduced in Section 2.5.

#### 2.2 Ionicity factor

Pauling (1960), Coulson *et al.* (1962), Phillips (1970, 1973), Christensen *et al.* (1987) and Garcia and Cohen (1993) have not determined ionicity factor of Rock-Salt and Wurtzite but they only focused on one physical property, i.e. the ionicity factor, of Wurtzite and Zinc-Blende.

The famous empirical ionicity factors are made by Pauling and Philips (Pauling, 1960). Pauling (1932) developed electronegativity X scale of the elements according to the relation given by

$$E(AB) = \frac{1}{2} [E(AA) + E(BB) + C(X_A - X_B)], \quad (2.1)$$

where  $E$  is referring to energy of  $AA$ ,  $BB$ , and  $AB$  bonds;  $X_A$ ,  $X_B$  are electronegativity of  $A$  and  $B$  atoms, respectively, and  $C$  is a constant for dimension of energy. Pauling (1932) had maintained that  $f_i(AB)$  must be an even function of  $X_A - X_B$  since it

measures the ionicity character and the value should be between zero and one. The conditions

$$f_i(AB) = f_i(BA), \text{ and } 0 \leq f_i(AB) \leq 1, \quad (2.2)$$

are satisfied by all ionicity factor definitions, including Pauling's definition. Pauling (1932) had developed ionicity factor of  $AB$  is given by

$$f_i(AB) = 1 - \exp\left[-\frac{1}{4}(X_A - X_B)^2\right]. \quad (2.3)$$

Later, Phillips (1970) had then stated that Pauling's definition in Equation (2.3) tends to make rough estimates of fraction for ionicity function,  $f_i(AB)$  on an  $AB$  bond. Based on Pauling's definition in Equation (2.3),  $f_i(AB)$  is a function of  $X_A$  and  $X_B$ , and independent with quantities of bond length. Pauling (1939) had developed the Equation (2.3) to include the ionicity factor of crystal as follows:

$$f_i = 1 - (N/M) \exp\left[-\frac{1}{4}(X_A - X_B)^2\right]. \quad (2.4)$$

In Equation (2.4),  $N$  is the number of the valence electrons, and  $M$  denotes the coordination of an  $A^N B^{8-N}$  crystal ( $N = 1, 2, 3, 4$  and  $M = 4$  or  $6$ ). The  $N/M$  factor reflects the increased ionic character of resonant bonds and takes into account the sharing of the  $N$  valence electrons by the  $M$  bonds (Pauling, 1960; Phillips, 1970).

Pauling (1960) had introduced an ionicity factor based on the electron negativity difference. According to ionicity factor definition by Pauling's (1960), there is a rough correlation between ionicity factor and dipole moments of diatomic molecules. The bond dipole moment uses the idea of electric dipole moment to measure the polarity of a chemical bond within a molecule. It occurs whenever there is a separation